

## HIGH TEMPERATURE PHASE EQUILIBRIA IN THE Ni-Al-Ta SYSTEM

P. Willemin<sup>\*</sup>, O. Dugué<sup>\*\*</sup>, M. Durand-Charre<sup>\*</sup>, J. Davidson<sup>\*\*</sup>

<sup>\*</sup>Institut National Polytechnique de Grenoble - L.T.P.C.M./E.N.S.E.E.G.  
B.P. 75 38402 SAINT MARTIN D'HERES, FRANCE

<sup>\*\*</sup>Département Etudes et Recherches, Imphy S.A., 58160 IMPHY, FRANCE

### Summary

Liquid-solid phase equilibria have been studied in the Ni-NiAl-Ni<sub>3</sub>Ta triangle of the Ni-Al-Ta system, using a combination of several experimental techniques. Five primary phases occur in this region, including the ternary compound Ni<sub>6</sub>TaAl which enters into equilibrium with each of the other four. Of the four invariant points, only one is a ternary eutectic. Compositions previously studied in the form of directionally aligned composites have been shown to contain Ni<sub>6</sub>TaAl and not Ni<sub>3</sub>Ta.

The work was carried out as part of a more extensive program whose ultimate aim is the calculation of complex superalloy phase diagrams. In the case of the Ni-Al-Ta ternary system, it has been shown that the liquidus surface in the primary  $\gamma$ -solid-solution phase field can be accurately described by a second order polynomial function of the atomic concentrations.

It is particularly desirable in the case of complex superalloy phase diagrams to be able to determine the limit of the primary  $\gamma$  solid-solution solidification field, together with liquidus, solidus and  $\gamma'$ -solvus temperatures. Such thermodynamic calculations must take into account all possible phases and in this respect the data obtained on the ternary compound Ni<sub>6</sub>TaAl should prove to be an especially important contribution.

### 1 - Introduction

The progressive improvement in the temperature capability of turbine blades obtained over the past 40 years has been achieved to a major extent by a gradual increase in the volume fraction of the hardening phase,  $\gamma'$ , in nickel-base superalloys, together with processing innovations such as columnar-grain and single-crystal casting. The trend has been retarded by the associated rise in  $\gamma'$  solvus and concomitant decrease in solidus temperature, rapidly leading to the appearance of eutectic  $\gamma'$ .

In order to counteract this tendency, there has been a shift in composition, many recent high-performance blade alloys being largely based on the Ni-Al-Ta system, with further additions, of which the most frequently employed are Cr and W. The use of Ta, in preference to Ti or Nb, leads to higher solidus temperatures and enables larger  $\gamma'$  volume fractions to be obtained without the formation of eutectic.

In spite of its practical importance, the Ni-Al-Ta system has been relatively little investigated, especially as regards the liquidus-solidus region. Nash and West (1), who studied solid-state phase equilibria at 1000°C and 1250°C in the region containing 50 to 100 at.% Ni, have briefly reviewed previous work. The currently accepted version of the Ni-Al binary system is that given by Hansen (2), and incorporates both a eutectic and a peritectic reaction close together, in the region of Ni<sub>3</sub>Al. After initial debate, these were situated on the nickel-rich side of  $\gamma'$ , following experiments carried out by Floyd (3). The Ni-Ta binary diagram given by Shunk (4) has been modified by Nash and West (5) who confirmed the formation in the solid state of Ni<sub>3</sub>Ta, first reported by Larson et al (6). This face-centered tetragonal compound is stable up to ~1300°C. In the three-component system, a pseudo-binary eutectic between Ni<sub>3</sub>Al ( $\gamma'$ ) and Ni<sub>3</sub>Ta (8), at 11.9 at.% Ta and 12.6 at.% Al has been reported, together with a ternary eutectic between  $\gamma$ ,  $\gamma'$  and  $\delta$  at 11.0 at.% Ta and 9.5 at.% Al (7). However, this does not concord with the existence of a ternary compound, Ni<sub>6</sub>TaAl, first recorded by Giessen and Grant (8) and subsequently confirmed by other workers (1,9). The melting point of this phase has been reported to be ~1530°C (9). Apart from a few isolated values (10), little information is available concerning the liquidus and solidus temperatures within the ternary system.

The aim of the present work was to improve understanding of the numerous liquid-solid transformations which occur in the nickel-rich part of the ternary phase diagram and to determine the limiting compositions compatible with the absence of phases other than  $\gamma$  or  $\gamma'$ . The investigations were therefore restricted to compositions within the triangle Ni-NiAl-Ni<sub>3</sub>Ta.

## 2 - Experimental procedure

### Materials

All alloys were prepared from high purity (> 99.95 %) materials. Small ingots of certain master-alloys were melted under argon in a medium-frequency induction furnace, while other, intermediate compositions were obtained by button-melting in an argon arc furnace ; in all a total of 52 alloys.

### Differential thermal analysis and quench-interrupted directional solidification

Phase transformation temperatures were determined by differential thermal analysis (DTA) on specimens of about 2g.

This technique was coupled with quench-interrupted directional solidification experiments (QDS) in which the solid-liquid interface configuration is frozen in by rapid cooling, enabling the solidification sequence to be determined. Another method employed was to monitor solidification occurring under controlled conditions in the DTA furnace and to quench the specimen at a precise moment, either on attainment of the liquidus surface or the appearance of a eutectic.

### Phase analysis

Phase analysis were carried out on an electron microprobe using accele-

rating voltages of 10 kV for Al and 20 kV for Ni and Ta, with application of a ZAF correction program. In the case of phases present in the form of fine particles, semi-quantitative analyses were also performed on a scanning electron microscope equipped with a solid-state detector.

Following a method which has been described elsewhere (11), wherever the microstructure allowed, it was particularly endeavoured to analyse the dendrite cores. In effect, when a QDTA specimen is quenched as soon as the first cooling peak is observed, the first solid is already formed and will be situated at the centre of the dendrites in the solidified microstructure. Since both the liquidus temperature and the liquid composition (that of the alloy) are known, analysis of the first-formed solid enables a tie-line to be determined. This is important since the solidification path commences in a direction defined by the liquidus conode.

### Phase identification

Phases were identified chiefly by X-ray diffraction of powdered samples. In a more limited number of cases X-ray diffraction was carried out by reflection on massive specimens, while other samples were investigated using electron diffraction on thin foils.

### Micrography

For a wide range of compositions, the variations in transformation temperatures were found to be only very slight, making it difficult, if not impossible, to determine the extent of the various liquidus regions from the DTA results alone. It was necessary to take into account the microstructural morphology, together with phase analyses and identifications. However, in many alloys the as-cast microstructure was modified by solid-state transformations, so that considerable care was required in interpretation. To illustrate this point, figures 1b and 1c represent the as-cast structure of alloy 7, while figure 1a shows the same alloy quenched immediately upon reaching the liquidus. Only in the latter case can the first-formed phase be identified unambiguously. After solidification at  $300^{\circ}\text{C.h}^{-1}$ , certain alloys showed similar microstructures to those illustrated in figure 1a, whereas different primary phases were identified in QDTA specimens (alloys 10 and 41).

By careful micrographical examination of interdendritic regions it was also possible to determine the solidification path and to deduce the direction and the nature of the univariant lines. This is illustrated in figure 2 for alloy 25, in which primary  $\gamma'$  dendrites are surrounded by  $\gamma + \gamma'$  eutectic, while both  $\text{Ni}_6\text{TaAl}$  ( $\pi$ ) and  $\delta$  phases are present in the light-etching interdendritic spaces. Figure 3, which represents a transverse section of a QDS specimen of alloy 13, is a further example and shows the convoluted morphology of the  $\gamma + \pi + \delta$  ternary eutectic formed from the last liquid to solidify.

## 3 - Results

Five phases have been identified within the triangle Ni-NiAl-Ni<sub>3</sub>Ta ;  $\gamma$ ,  $\gamma'$ ,  $\delta$ ,  $\beta$  and  $\text{Ni}_6\text{TaAl}$ , which has been called  $\pi$ . The crystal structures and lattice parameters are given in table I, together with values from the literature. The phase compositions corresponding to the parameters determined in the present investigation are as follows :

$\text{Ni}_{0.76}\text{Al}_{0.13}\text{Ta}_{0.09}$   $a = 0.3608\text{nm}$  ;  $\text{Ni}_{0.75}\text{Al}_{0.18}\text{Ta}_{0.07}$   $a = 0.3609\text{nm}$  ;  
 $\text{Ni}_{0.76}\text{Al}_{0.10}\text{Ta}_{0.14}$   $a = 0.5131\text{nm}$   $c = 0.8362\text{nm}$ . The phase transformation temperatures and the phases which may appear during solidification are listed in table II.

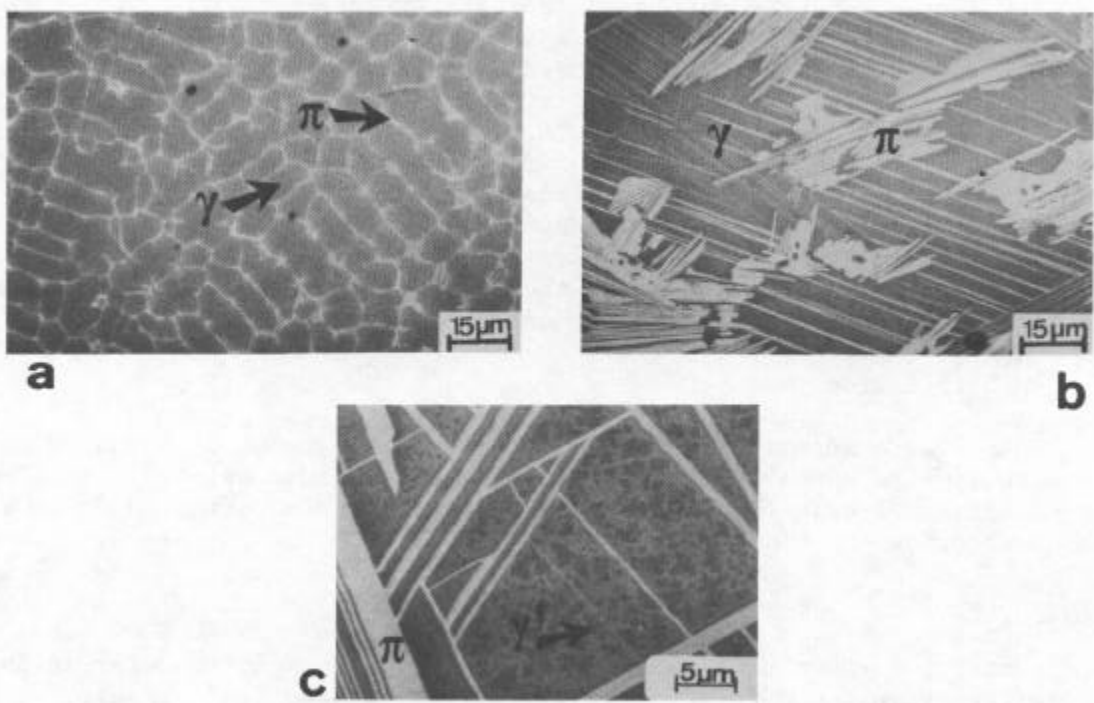


Figure 1 - Scanning electron micrographs of alloy 7 (Table II) E (Fig.5)  
 a) quenched from the liquidus      b) and c) cooled at 300 K.h<sup>-1</sup>

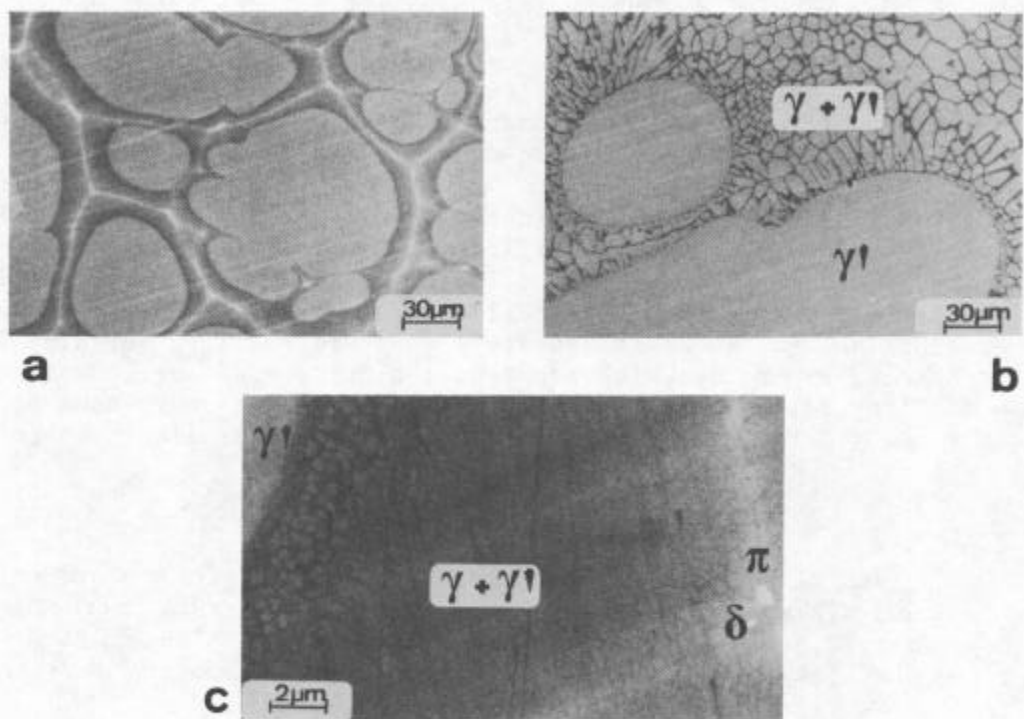


Figure 2 - Scanning electron micrographs of alloy 25 (Table II), J (Fig. 5)  
 a) quenched from the liquidus      b) and c) cooled at 300 K.h<sup>-1</sup>

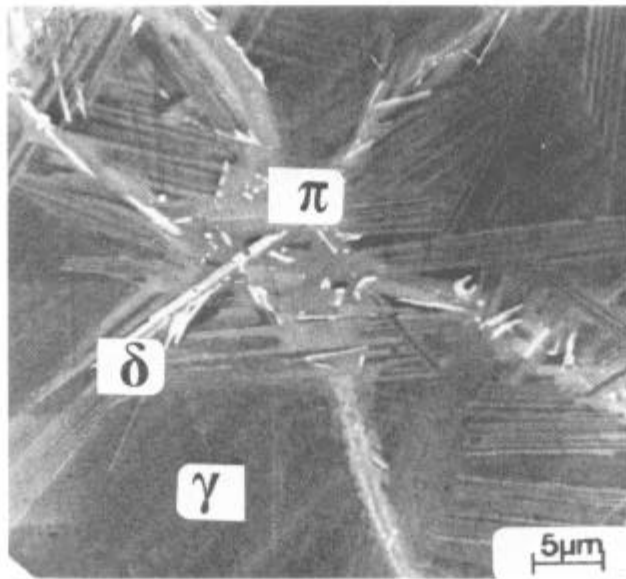


Figure 3 - Scanning electron micrograph of alloy 13 (Table II), M (Fig. 5). Transverse section of QDS specimen.

Table I. Crystal structures and lattice parameters of  $A_3B$  phases in the Ni-Al-Ta system

Equivalent Ni-base compound	$Ni_3Al$	$Ni_6TaAl$	$Ni_3Ta$	$Ni_3Ta$	$Ni_3Ta$
Phase type	$Cu_3Au$	$Ni_3Ti$	$Al_3Ti$	$Pt_3Nb$	$Cu_3Ti$
Bravais lattice	simple cubic	hexagonal	body centered tetragonal	monoclinic	orthorhombic
Lattice parameters in nm	$a=0.3573$ (1) $a=0.3607$ (1) $a=0.3608$ ★ $a=0.3609$ ★	$a=0.5112$ $c=0.8357$ (1) $a=0.5137$ $c=0.8366$ (9) $a=0.513$ $c=0.8362$ ★ $a=0.5112$ $c=0.8340$ (8)	$a=0.3571$ $c=0.7452$ (1) $a=0.3627$ $c=0.7455$ (13)	$a=0.511$ $b=0.454$ (8) $c=2.550$ (8) $\alpha=90^\circ 38'$ $a=0.512$ $b=0.452$ (13) $c=2.537$ $\alpha=90^\circ 50'$	$a=0.5117$ $b=0.4247$ (1) $c=0.4527$ $a=0.512$ $b=0.423$ (13) $c=0.452$ $a=0.514$ $b=0.4250$ (13) $c=0.4542$

★ present results      ( ) see list of references

Table II. Transformations temperatures and phases formed during solidification in the order of appearance

ALLOY NUMBER	COMPOSITION at %		TEMPERATURES T° C	PHASES FORMED
	balance			
	Al	Ni Ta		
1	5.1	6.7	1392	γ
2	15.3	2	1407, 1398	γ, γ'
3	14.1	3	1401, 1377	γ, γ'
4	13	4	1394, 1373	γ, γ'
5	11.2	6	1390, 1371	γ, γ'
6	8	10	1371, 1363	γ, π, δ
7	8	11	1368, 1358	γ, π
8	7	11	1370, 1355	γ, π
9	8.4	11.2	1373	γ, π
10	8.7	11.6	1372, 1365	γ, π, δ
11	6.4	13.4	1386, 1376, 1372	γ, δ, π
12	4.0	12.0	1384	γ
13	5.1	14.8	1427, 1386	γ, δ
14	7	8	1388	γ
15	5	8	1397	γ
16	3	8	1417	γ
17	8.3	3	1429	γ
21	19.9	2	1370	γ', γ
22	20.7	2.9	1376, 1362	γ', γ
23	19	4	1380, 1370	γ', γ
24	18.4	4	1388, 1365	γ', γ
25	15.2	6	1381, 1368	γ', γ, π, δ
26	17.3	6.7	1390, 1387	γ', γ
27	18	7	1402	γ', π, δ, β
28	15.9	9.1	1398, 1386	γ', π, δ, β
29	14.8	11.1	1380, 1374, 1324	γ', π, δ, β
30	13.1	8.7	1383, 1365	γ', π, γ, δ
31	12	8	1375, 1368	γ', γ, π, δ
41	9.1	12.6	1375, 1360	π, γ, δ
42	10.2	13.7	1383, 1378	π, δ, β
43	10.4	14.4	1390, 1387	π, δ, β
44	12.6	12.7	1390, 1384	π, β, δ
45	13.3	12	1393, 1388	π, γ', β, δ
61	12	16	1400, 1377, 1308	δ, π, β
62	8.6	19.7	1465, 1326	δ, β
63	0	22	1496, 1376	δ, γ
64	4.7	19.7	1498, 1405, 1321	δ, π, β
65	3.71	15.53	1439, 1385, 1377	δ, γ, π
66	15.30	14.60	1376, 1310	δ, β
67	2.7	15.3	1423, 1384	δ, γ, π
81	32.2	2.3	1402, 1382	β, γ', δ
82	27.6	9.7	1446, 1316	β, δ
83	19.8	10.7	1374, 1347, 1333	β, γ', π, δ
84	17.2	11.75	1380, 1356, 1336	β, γ', π, δ
85	19.3	12.9	1341, 1336, 1310	β, γ, π, δ

The liquidus temperatures vary very little for alloys containing between 75 and 80 at.% Ni and more than 7 at.% Al, being in the range ~ 1390 to 1400°C. This is illustrated in figure 4 which shows the vertical section of the liquidus along the line Ni<sub>3</sub>Al-Ni<sub>3</sub>Ta

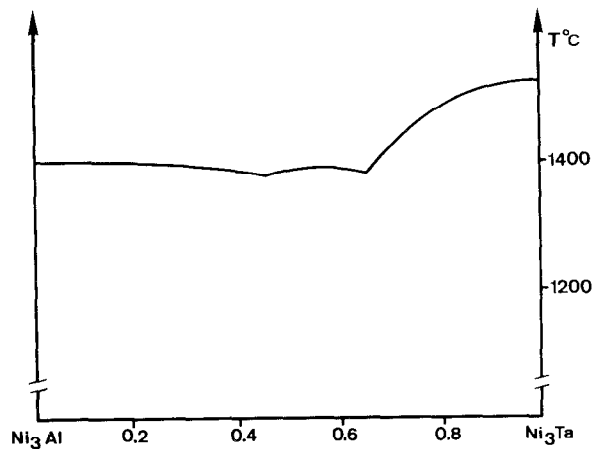


Figure 4 - Vertical section through the liquidus between Ni<sub>3</sub>Al and Ni<sub>3</sub>Ta

The liquidus surface in the primary  $\gamma'$  solid-solution phase field has been represented by a second-order polynomial function of the atomic concentrations of each constituent element. The coefficients in this equation were determined by a least squares fitting technique, using 18 experimentally determined values. The following expression was obtained :

$$T = 1453 + 348 x_{Al} - 1033 x_{Ta} - 3052 x_{Al}^2 - 2945 x_{Al} x_{Ta} + 4046 x_{Ta}^2$$

T : Temperature °C                      x : atom % content.

The discrepancy between the experimental values and those calculated from the above relation is less than 4K, which is the order of magnitude of the overall precision of the liquidus measurements.

Figure 5 represents the projection of the liquidus surface for the Ni-NiAl-Ni<sub>3</sub>Ta triangle. It shows the primary solidification fields for each phase. In the nickel-rich corner, an extensive  $\gamma$  solid-solution region is bordered by three fields corresponding to the A<sub>3</sub>B phases  $\gamma'$ ,  $\pi$  and  $\delta$ .

Table III gives the ranges of composition determined for each of the primary phases and shows that the  $\delta$ -phase dissolves very little aluminium, while, the solubility of Ta in the  $\beta$ -phase is also small. On the contrary,  $\gamma$ ,  $\gamma'$  and  $\pi$  phases have considerable solubility ranges in the solid-liquid region.

It was not always possible to determine with certainty the nature of the univariant lines. Most of them appear to be of the eutectic type. However the line p1-4 apparently maintains its peritectic character up to the invariant point 4, while the line e3-3 may possibly become peritectic before reaching the junction 3. The nature of the invariant reaction is likewise uncertain except for point 2 which is clearly a ternary eutectic. The eutectic line between  $\beta$  and  $\delta$  falls away towards lower Ni contents and probably meets the Ni-Ta field, since this phase has been identified in the interdendritic spaces of certain alloys, such as n° 62 and n° 65.

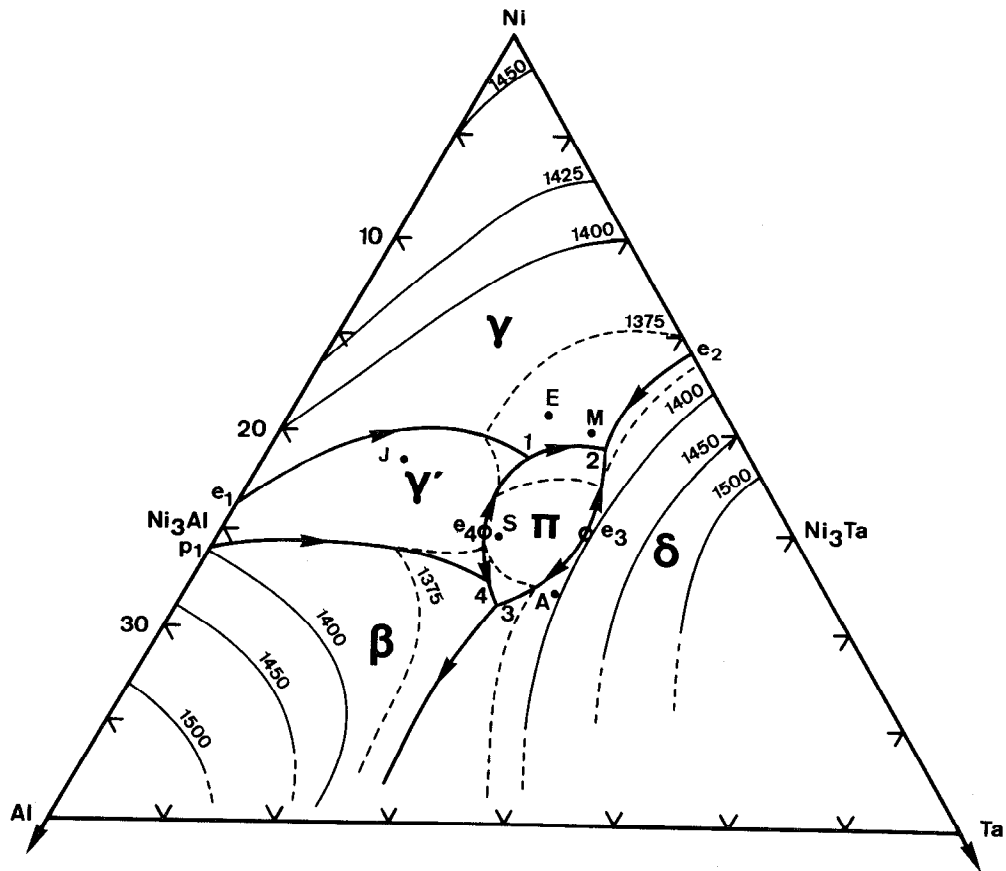


Figure 5 - Liquidus surface and univariant lines in the Ni-NiAl-Ni<sub>3</sub>Ta triangle.

Table III. Limiting compositions of primary phases

Phase	Composition (at.%)		
	Al	Ta	Ni
π	8 to 12	13.5 to 14.5	70 to 80
δ	0 to 2.5	23.5 to 25	70 to 85
β	35 to 45	0 to 3	50 to 75
γ'	7 to 25	0 to 10	75 to 80
γ	0 to 15	0 to 15	80 to 100



The vertical section through  $\text{Ni}_3\text{Ta}$  and  $\text{Ni}_3\text{Al}$  can be considered approximately to be a quasi-binary system, at least in its central part, since the univariant lines descend on each side of it. This has been established by the observation that the solidification paths of alloys with greater than 75 at.% Ni terminate with the formation of the ternary eutectic  $\delta + \pi + \gamma$ , whereas for alloys with lower Ni contents they end with a characteristic  $\beta + \delta$  eutectic, figure 6.

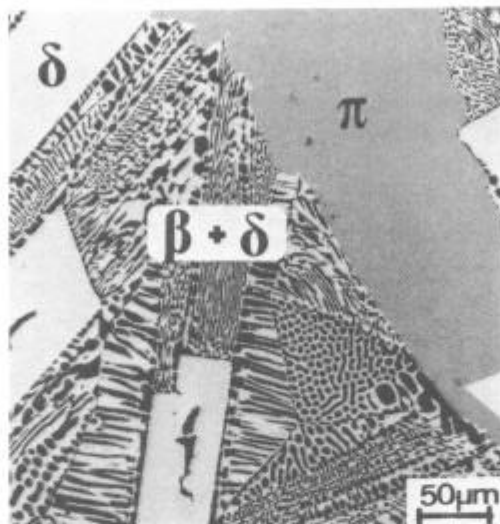


Figure 6 - Scanning electron micrograph of alloy 61 (Table II), A (Fig. 5), cooled at  $300 \text{ K.h}^{-1}$

Most of the primary phases show signs of solid-state transformations. In the  $\gamma$  phase, precipitation of  $\gamma'$  with a typical cuboidal or dendritic morphology is common, while the  $\pi$  phase tends to form laths in certain preferred directions. Figure 1 shows both  $\gamma'$  and  $\pi$  phases precipitated from the primary  $\gamma$ . Laths of  $\gamma$  have been identified in areas of primary  $\pi$ -phase and laths of  $\delta$  in primary  $\beta$ , the precipitation being of the Widmanstätten type.

#### 4 - Discussion and conclusions

The present work has shown the importance of combining several different techniques for the study of complex liquid-solid equilibria. Micrography and micro-analysis are essential, but great care must be taken in interpreting microstructures. In particular, QDS and QDTA proved to be especially useful for avoiding misleading solid-state transformations.

The major difficulty encountered was the extreme flatness of certain parts of the liquidus surface. In these areas, transformation temperatures alone were of little help in determining the solidification sequences and had to be completed by a considerable amount of micro-analysis and phase identification.

The results are in overall agreement with the isothermal sections determined in the solid state by Nash and West (1), essentially by X-ray diffraction studies. In particular, the existence of a ternary compound,  $\text{Ni}_6\text{TaAl}$ , has been confirmed. However, its congruent melting point was found to be  $\sim 1400^\circ\text{C}$  and not  $\sim 1530^\circ\text{C}$  as proposed by Mints et Al. (9). The formation of this phase, designated here as  $\pi$ , was overlooked by Hubert and his co-

workers (7,12) who sought structures capable of yielding directionally aligned composites. The present investigation shows that the pseudo-binary eutectic which they described as  $\gamma' + \delta$  is in fact  $\gamma' + \pi$ , figure 7, while their ternary eutectic  $\gamma + \gamma' + \delta$  corresponds in reality to an invariant reaction between liquid,  $\gamma'$ ,  $\gamma + \pi$ . Their assumption that the section Ni<sub>3</sub>Al-Ni<sub>3</sub>Ta represents a quasi-binary system has been shown to be only partly correct. It cannot of course be so on the Ni-Al binary side, since Ni<sub>3</sub>Al does not melt congruently.

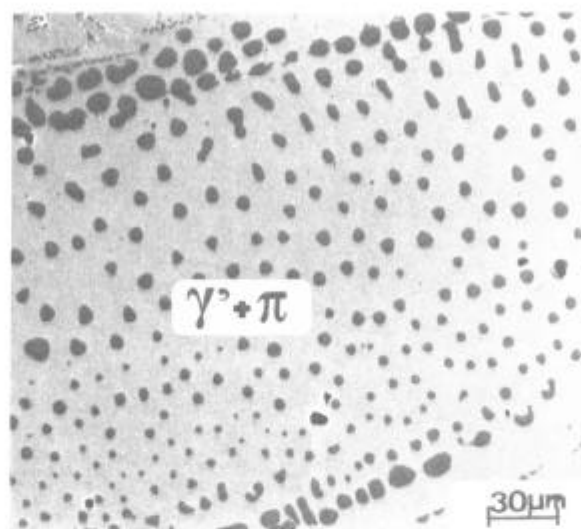


Figure 7 - Scanning electron micrograph of alloy 45 (Table II), S (Fig. 5), cooled at  $300 \text{ K.h}^{-1}$  and showing the  $\gamma' + \pi$  eutectic. The dark phase is  $\gamma'$ .

The work described in the present paper was carried out as part of a more extensive program whose ultimate aim is to calculate complex superalloy phase diagrams, and in particular to determine the limit of the primary  $\gamma$  solid-solution solidification field, together with liquidus, solidus and  $\gamma'$ -solvus temperatures. Such thermodynamic calculations must take into account all possible phases and in this respect the data obtained on the ternary compound Ni<sub>6</sub>TaAl should prove to be an especially important contribution.

#### References

- (1) P. Nash, D.R.F. West, "Phase equilibria in the Ni-Ta-Al system", *Met. Sci.* 13 (1979) 670-676.
- (2) M. Hansen, K. Anderko, "Constitution of binary alloys", 2nd ed., (1958) New York (Mc Graw-Hill).
- (3) R.W. Floyd, "The constitution of nickel-rich alloys of the nickel-chromium-aluminium system", *J. Inst. Met.* 80 (1951-2) 551-553.
- (4) F.A. Shunk, "Constitution of binary alloys, 2nd supplement" (1959) ; New York (Mc Graw-Hill).
- (5) P. Nash, D.R.F. West, "Ni-Al and Ni-Ta phase diagrams", *Met. Sci.* 17 (1983) 99-100.
- (6) J.M. Larson, R. Taggart, D.H. Polonis, "Ni<sub>6</sub>Ta in nickel rich Ni-Ta alloys", *Met. Trans.* 1 (1970) 485-489.

- (7) F. Mollard, B. Lux, J.C. Hubert, "Directionally solidified composites based on the ternary eutectic Ni-Ni<sub>3</sub>Al-Ni<sub>3</sub>Ta", Z. Metallkunde 65 (1974) 461-468.
- (8) B.C. Giessen, N.J. Grant, "New intermediate phases in transition metal systems", Acta Cryst. 18 (1965) 1080-1081.
- (9) R.S. Mints, N.P. D'Yakonova, Ya.S. Umanskii, Yu.A. Bondarenko, T.A. Bondarenko, "Interactions of the phases Ni<sub>3</sub>Al and Ni<sub>3</sub>Ta", Sov. Phys. Dokl. 17 (1973) 904-906.
- (10) P.W. Peterson, T.Z. Kattamis, A.F. Giamei, "Coarsening kinetics during solidification of Ni-Al-Ta dendritic monocrystals", Met. Trans. A, 11A (1980) 1059-1065.
- (11) M. Durand-Charre, N. Valignat, F. Durand, "Méthode expérimentale pour évaluer l'influence de chaque élément sur les microségrégations de solidification dans les alliages complexes : application à une gamme d'alliages (Fe, Ni, Co, Al, Ti), Mém. Sci. Rev. Mét. (janvier 1979) 51-62.
- (12) J.C. Hubert, W. Kurz, B. Lux, "Croissance en solidification dirigée de l'eutectique quasi-binaire Ni<sub>3</sub>Al-Ni<sub>3</sub>Ta", J. Crystal Growth 13-14 (1972) 757-764.
- (13) B.C. Giessen, N.J. Grant, "The crystal structure of TaNi<sub>3</sub> and its change on cold working", Acta Met. 15 (1967) 871-877.